Atmos. Chem. Phys., 24, 4411–4419, 2024
https://doi.org/10.5194/acp-24-4411-2024

Atmospheric Chemistry and Physics
Open Access
EGU

Technical Note: A technique to convert NO_2 to NO_2^- with S(IV) and its application to measuring nitrate photolysis

Aaron Lieberman, Julietta Picco, Murat Onder, and Cort Anastasio

Department of Land, Air, and Water Resources, University of California – Davis, Davis, California 95616, United States

Correspondence: Cort Anastasio (canastasio@ucdavis.edu)

Received: 1 December 2023 – Discussion started: 4 December 2023
Revised: 23 February 2024 – Accepted: 26 February 2024 – Published: 16 April 2024

Abstract. Nitrate photolysis is a potentially significant mechanism for "renoxifying" the atmosphere, i.e., converting nitrate into nitrogen oxides – nitrogen dioxide (NO_2) and nitric oxide (NO) – and nitrous acid (HONO). Nitrate photolysis in the environment occurs through two channels which produce (1) NO_2 and hydroxyl radical (•OH) and (2) nitrite (NO_2^-) and an oxygen atom ($O(^3P)$). Although the aqueous quantum yields and photolysis rate constants of both channels have been established, field observations suggest that nitrate photolysis is enhanced in the environment. Laboratory studies investigating these enhancements typically only measure one of the two photo-channels, since measuring both channels generally requires separate analytical methods and instrumentation. However, measuring only one channel makes it difficult to assess whether secondary chemistry is enhancing one channel at the expense of the other or if there is an overall enhancement of nitrate photochemistry. Here, we show that the addition of S(IV), i.e., bisulfite and sulfite, can convert NO_2 to NO_2^-, allowing for measurement of both nitrate photolysis channels with the same equipment. By varying the concentration of S(IV) and exploring method parameters, we determine the experimental conditions that quantitatively convert NO_2 and accurately quantify the resulting NO_2^-. We then apply the method to a test case, showing how an •OH scavenger in solution prevents the oxidation of NO_2^- to NO_2 but does not enhance the overall photolysis efficiency of nitrate.

1 Introduction

Nitrogen oxides – i.e., nitrogen dioxide (NO_2) and nitric oxide (NO) – and nitrous acid (HONO) are reactive species that play key roles in the formation of tropospheric ozone and hydroxyl radicals (•OH) (Acker et al., 2006; Seinfeld and Pandis, 2006). The fast oxidation of NO_2 to HNO_3 is an important sink of gas-phase NO_x, while the resulting gas-phase nitric acid and aqueous nitrate are traditionally considered relatively stable reservoir species (Stavrakou et al., 2013; Ye et al., 2017). Although nitrate can photolyze to re-form NO_x, the lifetime of nitrate is long enough that the small production rates of NO_x and HONO from nitrate photolysis have been considered important only in remote areas (Romer et al., 2018). However, field studies over the past several decades have often shown that atmospheric measurements of HONO and NO_x are higher than modeled values (Li et al., 2014; Zhou et al., 2002; Romer et al., 2018). This suggests that nitrate photolysis in the atmosphere is faster than originally considered and, therefore, might be a more significant source of HONO and NO_x (Kasibhatla et al., 2018; Andersen et al., 2023; Zhou et al., 2003).

In sunlight (i.e., for wavelengths above 280 nm), aqueous NO_3^- photolysis proceeds through two channels:

$$NO_3^- + h\nu \rightarrow NO_2 + {\bullet}O^-, \quad \text{(R1)}$$

$$NO_3^- + h\nu \rightarrow NO_2^- + O\left(^3P\right). \quad \text{(R2)}$$

The first channel (Reaction R1) produces NO_2 and $\bullet O^-$ (which is rapidly protonated to •OH), and the second produces nitrite (NO_2^-) and an oxygen atom $O(^3P)$. Channel 1 has an average quantum yield of (1.19 ± 0.29) % at 293 K for

illumination wavelengths above 300 nm (Chu and Anastasio, 2003; Zellner et al., 1990; Warneck and Wurzinger, 1988; Zepp et al., 1987), as shown in Table S1 in the Supplement. The quantum yield for channel 2 (Reaction R2) is sometimes erroneously reported to be an order of magnitude smaller than that of channel 1, but in fact the values are comparable: channel 2 has an average quantum yield of (0.98 ± 0.11) % at 293 K for wavelengths above 300 nm (Benedict et al., 2017; McFall et al., 2018; Warneck and Wurzinger, 1988; Goldstein and Rabani, 2007) (Table S1).

These two quantum yields have been determined using different analytical methods. Generally, researchers either monitor the production of hydroxyl radical (•OH) from channel 1 or the production of nitrite (NO_2^-) from channel 2. •OH is typically quantified using a chemical probe (e.g., benzoic acid) that reacts to form a stable product (e.g., *p*-hydroxybenzoic acid) that is monitored by high-performance liquid chromatography (HPLC) (Chu and Anastasio, 2003). In contrast, NO_2^- is typically measured via ion chromatography or the more sensitive long-path Griess method that derivatizes nitrite and measures the highly colored azo product (Benedict et al., 2017; Ridnour et al., 2000).

Other studies have measured the gas-phase production of NO_2 and/or HONO, which is formed from the protonation of NO_2^-. However, these gas-phase studies are limited to a specific pH range in order to measure HONO production (Scharko et al., 2014), employ separate instruments to measure HONO and NO_2, and focus on how the production rates of NO_2 and HONO depend on experimental conditions (Frey et al., 2013; Ma et al., 2021; Liang et al., 2021). Although it is possible to measure both NO_x and HONO with commercially available instruments, researchers often engineer their own instrument to measure HONO and operate a second analyzer for the NO_2 channel (Shi et al., 2021; X. Wang et al., 2021; Ma et al., 2021). Furthermore, gas-phase studies do not measure quantum yields but instead examine how the production rates of NO_2 and/or HONO are altered by factors such as the presence of other chemical species.

Typically researchers define an enhancement in nitrate photolysis as an experimentally measured production rate or quantum yield divided by the value under a standard condition (Liang et al., 2021; Y. Wang et al., 2021; Shi et al., 2021; Zhou et al., 2003). For example, a measured apparent nitrite quantum yield of 8 % in the presence of light-absorbing vanillic acid (Y. Wang et al., 2021) represents an 8-fold enhancement. If we want to fully understand the impact of an enhancement, the quantum yields for both channels must be measured. For instance, if one measures only the NO_2 channel and discovers an enhanced formation rate, it would be unclear whether NO_2^- production also increased or if NO_2^- is being converted to NO_2. Therefore, it would be useful to be able to measure both channels of nitrate photolysis using a single analytical method.

One possible method to measure both channels is by reducing NO_2 to NO_2^- after photolysis, such that the total measured NO_2^- is the combination of NO_2 from channel 1 and NO_2^- from channel 2. S(IV) – i.e., sulfite (SO_3^{2-}) and bisulfite (HSO_3^-) – can reduce NO_2 to NO_2^- through the following overall reaction (Lee and Schwartz, 1982; Clifton et al., 1988; Wang et al., 2020; Song et al., 2021):

$$2NO_2 + HSO_3^- + H_2O \rightarrow 2NO_2^- + 3H^+ + SO_4^{2-}. \quad \text{(R3)}$$

Although industrial processes have used this reaction to convert NO_2 to NO_2^-, they often operate at very high temperatures or include additives to enhance the diffusion of NO_2 into the aqueous phase (Shen and Rochelle, 1998; Lian et al., 2022).

Our goal is to use S(IV) chemistry to determine both channels of nitrate photolysis by performing two experiments using the same analytical method. In the first run, we measure NO_2^- production directly to quantify channel 2. In the second experiment, we use S(IV) to convert photoproduced NO_2 to NO_2^- so that the measured nitrite represents the sum of both NO_2 and NO_2^-. Then we quantify channel 1 by subtracting the NO_2^- experiment result from the combined ($NO_2 + NO_2^-$) experiment result. If this approach is successful, it would simplify and expand our ability to analyze NO_2 and NO_2^-.

2 Methods

2.1 Materials

Information about materials and chemicals is in Sect. S1 of the Supplement.

2.2 Sample illumination

Illumination solutions were prepared daily; were air saturated; and contained 50 µM $NaNO_3$, either 0 or 50 µM 2-propanol, and varying concentrations of S(IV). The pH of the solution was either controlled by a 0.010 M phosphate buffer (pH 5 or 8) or the added S(IV) (pH 8). Samples were illuminated with 313 nm light from a 1000 W mercury–xenon arc lamp with a downstream monochromator (Spectral Energy) and a 310 nm long-pass filter upstream of the sample. A volume of 800 µL of aqueous sample in an upright 2 mL HPLC vial (low impurity type-I class-A borosilicate glass, 12 mm o.d. × 32 mm height, Shimadzu) sealed with a septum cap was illuminated from its side. Samples were illuminated with constant stirring in a custom-built, Peltier-cooled aluminum housing (Paige Instruments) that was held at 20 °C by a recirculating water bath. Samples were kept sealed throughout the illumination. Dark controls containing the same solution as the illuminated sample but not exposed to light were analyzed periodically throughout each experiment. Nitrite production was never detected in the dark controls. Under our conditions, experiments without S(IV) produced no more than 180 nM NO_2^-, and experiments with S(IV) produced no more than 180 nM $NO_2 + NO_2^-$.

2.3 Measurement of nitrite

After illuminating all the samples for a given experiment, we determined nitrite concentrations using the Griess method, a spectrophotometric technique that forms an azo-dye complex (Doane and Horwath, 2003; Benedict et al., 2017; McFall et al., 2018). Our experiments had three different sample treatments: (1) no S(IV) in solution, (2) S(IV) in solution during illumination, and (3) S(IV) added to the solution after illumination. Each treatment required a slightly different method to efficiently form the azo dye. The stabilities of the samples are discussed in Section S3 of the Supplement.

For samples without S(IV), the Griess method (Pratt et al., 1995; Moorcroft et al., 2001; Ridnour et al., 2000; Benedict et al., 2017) could be used without adaptation. Within 10 min of stopping illumination, we added 25 µL of a 1% sulfanilamide in 10 % HCl (v/v) solution, and we let it react for 10 min in the dark. We then added 25 µL of 0.1 % N-(1-naphthyl)ethylenediamine dihydrochloride (NED) solution and allowed it to react for 10 min to form the azo dye.

Treatment 2, where S(IV) was present in solution during illumination, required an additional step because S(IV) interferes with the Griess reagents (Sect. S2). After illumination, we first added hydrogen peroxide (H_2O_2) to the 800 µL sample to obtain a 2 : 1 molar ratio of H_2O_2 : S(IV). This was done to oxidize S(IV) to sulfate, which does not interfere with nitrite determination. Within 1 min of adding H_2O_2, we added 50 µL of 1 % sulfanilamide in 30 % (v/v) HCl solution and allowed the solution to react for 10 min in the dark. Then we added 50 µL of 0.1 % NED solution to the sample and allowed it to react for another 10 min in the dark.

Treatment 3 is similar to treatment 2 with one key difference: S(IV) was added to the solution after illumination. Because NO_2 is volatile and would escape the illumination container if opened, we developed a method to add the S(IV) without opening the vial. This was done by using a syringe with a hypodermic needle to directly inject 37.5 µL of a 33.3 mM sulfite solution at pH 9 through the septum into the HPLC vial immediately after the illumination was stopped. The vial was then left to react while stirring for 30 min in the dark at room temperature to completely convert NO_2 to NO_2^-. The samples were then treated exactly as in treatment 2, i.e., adding H_2O_2, then 50 µL of sulfanilamide in 30 % HCl, and then 50 µL of NED.

Once the azo dye was formed, we measured light absorption at ∼ 540 nm in the developed solutions using a TIDAS II spectrophotometer (World Precision Instruments) with a liquid waveguide capillary cell (LWCC; nominal length of 100 cm, effective path length of 94 cm, 250 µL volume) and a tungsten lamp. The TIDAS contains two lamps, but the deuterium lamp (200–350 nm) caused an artifact in previous experiments (Benedict et al., 2017), so it was kept off during our measurements. The absorption spectrum was measured from 350 to 700 nm so that we could correct for any baseline shifts. The peak height between 530 and 550 nm was determined as the difference between the maximum absorbance in this range relative to a baseline drawn from the local absorption minima between 400 and 500 nm and between 550 and 700 nm. The limits of detection for nitrite were 7 nM for sample treatment 1 and 11 nM for sample treatments 2 and 3, as determined using the method of Armbruster and Pry (2008). Fresh standards of sodium nitrite (0 to 200 nM) were prepared daily and used to calibrate the spectrophotometer. As S(IV) and H_2O_2 decrease the absorbance, S(IV) and H_2O_2, respectively, used in the samples were also added to the standards to correct for this matrix effect. Samples and other solutions were manually injected into the LWCC with a syringe, and 4 mL of Milli-Q water was injected between samples to eliminate carry over. We cleaned the LWCC both before and after each experiment with 1 mL injections of three separate cleaning solutions: 1 M NaOH, 1 M HCl, and 50 % methanol with 50 % Milli-Q (MQ) water, with pure MQ injected between each cleaning solution.

Daily controls included a replicate standard, MQ injection as a check for carry over, and a secondary check standard (Dionex). Analyses were deemed acceptable if the MQ check was below the lowest non-zero standard (10 nM NO_2^-) and if both the replicate standard and secondary check standard concentrations were within 15 % of known values.

2.4 Chemical actinometry and calculation of quantum yield

The photon flux was measured daily using 2-nitrobenzaldehyde (2NB) as a chemical actinometer (Galbavy et al., 2010). Actinometry was performed under the same conditions (container, volume of sample, temperature) as nitrate photolysis. Under low-light-absorbing conditions, the measured rate constant for 2NB loss during 313 nm irradiation ($j_{2NB,313}$) is calculated using

$$j_{2NB,313} = 2.303 \times 10^3 \left(I_{313}l\right)\left(\varepsilon_{2NB,313}\phi_{2NB,313}\right), \quad (1)$$

where $I_{313}l$ is the surface-area-normalized photon flux (mol photon cm^{-2} s^{-1}), $\varepsilon_{2NB,313}\phi_{2NB,313} = 640\ M^{-1}\ cm^{-1}$ is the product of the base-10 molar absorption coefficient and quantum yield for 2NB at 313 nm (Anastasio et al., 1994), 2.303 converts ε to base-e, and $10^3\ cm^3\ L^{-1}$ is for units conversion. Similarly, the formation rate constant for nitrite from nitrate photolysis is

$$j\left(NO_3^- \rightarrow NO_2^-\right)_{313} = 2.303 \times 10^3 \left(I_{313}l\right)\left(\varepsilon_{NO_3^-,313}\right)\left(\phi\left(NO_2^-\right)_{313}\right), \quad (2)$$

where $\phi(NO_2^-)_{313}$ is the quantum yield of nitrite formation from nitrate photolysis at 313 nm, and $\varepsilon_{NO_3^-,313}$ is the base-10 molar absorption coefficient of nitrate at 313 nm, i.e., $5.29\ M^{-1}\ cm^{-1}$ (Chu and Anastasio, 2003).

The rate of nitrite formation from nitrate photolysis, $d[NO_2^-]/dt$, is a first-order process:

$$\frac{d\left[NO_2^-\right]}{dt} = j\left(NO_3^- \rightarrow NO_2^-\right)_{313}\left[NO_3^-\right]. \quad (3)$$

Since the experiments were at short timescales where nitrate loss was negligible, the increase of nitrite was linear, and the nitrite formation rate could be determined with simple linear regression. Combining Eqs. (1)–(3) allows us to solve for the quantum yield of nitrite:

$$\phi\left(NO_2^-\right)_{313} = \frac{d\left[NO_2^-\right]}{dt} \times \frac{\varepsilon_{2NB,313}\phi_{2NB,313}}{j_{2NB,313}\varepsilon_{NO_3^-,313}}\left[NO_3^-\right]. \quad (4)$$

For simplicity, and because all our experiments were performed with 313 nm illumination, we omit the "313" subscript throughout the rest of this article.

2.5 Combined quantum yield and $\phi(NO_2)$ calculations

For experiments with added S(IV), the measured concentration of nitrite represents both the primary nitrite from nitrate photolysis as well as secondary nitrite formed by conversion of NO_2. Thus, the calculated quantum yield in experiments with S(IV), i.e., $\phi(NO_2^-)_{S(IV)}$, is a combination of the quantum yields for both channels 1 and 2:

$$\phi\left(NO_2^-\right)_{S(IV)} = \phi\left(NO_2^-\right) + f \times \phi\left(NO_2\right). \quad (5)$$

Here f is the fraction of NO_2 that reacts with S(IV) to make NO_2^-, as opposed to going down other pathways:

$$f = \frac{k_{HSO_3^-+NO_2} \times \left[HSO_3^-\right] + k_{SO_3^{2-}+NO_2} \times \left[SO_3^{2-}\right]}{k_{HSO_3^-+NO_2} \times \left[HSO_3^-\right] + k_{SO_3^{2-}+NO_2} \times \left[SO_3^{2-}\right] + k_{other}} \quad (6)$$

where $k_{S(IV)+NO_2}$ is the reaction rate constant of S(IV) and NO_2, i.e., $1.2\times10^7\ M^{-1}\ s^{-1}$ and $1.7\times10^7\ M^{-1}\ s^{-1}$ for bisulfite and sulfite, respectively (Clifton et al., 1988), and k_{other} is the pseudo-first-order rate constant for all other pathways that consume NO_2. The concentrations of bisulfite and sulfite are determined based on the total S(IV) in solution, [S(IV)], and their mole fractions, which depend on the two pK_a values for S(IV) ($pK_{a_1} = 1.9$, $pK_{a_2} = 7.2$; Seinfeld and Pandis, 2006). As described below, at pH $\approx$ 8, a S(IV) concentration of 1.5 mM and higher is sufficient to make f equal 1; that is, S(IV) is essentially the only fate for NO_2, so it is quantitatively converted to NO_2^-. Under this condition, we calculate the quantum yield for NO_2 formation, $\phi(NO_2)$, as the difference between the measured nitrite quantum yields in the presence and absence of S(IV):

$$\phi\left(NO_2\right) = \phi\left(NO_2^-\right)_{S(IV)} - \phi\left(NO_2^-\right). \quad (7)$$

3 Results

3.1 Modification of the Griess method for solutions containing S(IV)

As described in Sect. S2, we found that the addition of micromolar levels of S(IV) interferes with the determination of nitrite because of two issues: (1) it prevents the formation of the azo-dye derivative, and (2) it moves the solution acidity out of the required range. The first issue was solved by oxidizing the S(IV) to S(VI) with H_2O_2 prior to the addition of the Griess reagents (Fig. S1 in the Supplement). We added H_2O_2 to the samples such that there was a 2 : 1 molar ratio of H_2O_2 : S(IV); then within 1 min of the addition of H_2O_2, we added the sulfanilamide solution and, 10 min later, the NED reagent. After waiting another 10 min, we measured the UV–VIS spectra for the entire batch of samples within 20 min of capturing the spectrum of the first sample. We also doubled the standard volumes of both Griess reagents added to the sample solutions to ensure that there were enough reactants to form the azo dye.

The second issue caused by S(IV) was that it pushed the solutions to pH 7. This basicity prevented the conversion of nitrite to the azo dye because this reaction requires a pH below 2. The standard 10 % HCl (v/v) in the sulfanilamide solution only lowered the sample pH to $\sim$ 4 for solutions containing 1.5 mM of sulfite. As per the recommendation by Doane and Horwath (2003), we increased the HCl concentration in the sulfanilamide solution to 30 % (v/v), which lowered the pH of the sample–sulfanilamide mixture to less than 2, overcoming the pH issue caused by S(IV).

3.2 Addition of S(IV) to solution prior to illumination

Our goals in this initial set of experiments were to examine whether S(IV) in solution can convert photoproduced NO_2 to NO_2^- and, if so, to determine the concentration of aqueous S(IV) required to make this conversion quantitative, i.e., close to 100 %. If S(IV) can quantitatively convert NO_2 to NO_2^-, then the measured nitrite quantum yield at this S(IV) concentration should equal the sum of the quantum yields from both channels of nitrate photolysis.

We started experiments by running a test without S(IV) (50 µM $NaNO_3$, 50 µM 2-propanol, and 293 K) to confirm that our result matches the literature. The average $\phi(NO_2^-)$ from our four replicate experiments without S(IV) is (1.05 $\pm$ 0.06) %, which is statistically no different ($p = 0.36$) from the average of the literature values shown in Table S1, (0.98$\pm$0.11) %. Then we began performing experiments with increasing concentrations of S(IV). As [S(IV)] increases, the apparent nitrite quantum yield increases until it reaches a plateau for S(IV) concentrations at roughly 500 µM and above (Fig. 1). The measured quantum yield at the plateau, determined as the average ($\pm1\sigma$) of the individual experiments from 500 to 2000 µM S(IV), is (2.01 $\pm$ 0.05) %. This

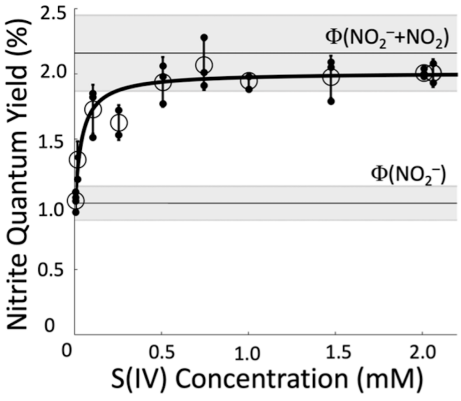

Figure 1. Measured apparent nitrite quantum yields for the photolysis of 50 µM nitrate solutions (293 K, pH 8) in the presence of different concentrations of S(IV). Unfilled circles represent the average ($\pm 1\sigma$) of individual experiments, which are shown as filled black points. The line through the data is a fit to Eq. (8). The lower grey area centered at 1.1 % is the average of previously determined values of $\phi(NO_2^-) \pm 1\sigma$, and the upper grey area centered at 2.2 % is the sum of the quantum yields from both channels, $\phi(NO_2^- + NO_2) \pm 1\sigma$, from the literature. Literature values used to calculate these averages are in Table S1.

is slightly lower than but statistically indistinguishable ($p = 0.14$) from the sum of the average literature quantum yields for both channels, (2.17 ± 0.52) %, which is shown as the upper horizontal line in Fig. 1. We then calculate $\phi(NO_2)$ by taking the difference between the quantum yield determined with S(IV), which measures the sum of the two channels, and the quantum yield for the nitrite channel (Eq. 7). This results in a value for $\phi(NO_2)$ of (0.96 ± 0.12) %, which is slightly lower than the average of previous experiments (1.19 ± 0.29) % but statistically no different ($p = 0.10$). These results confirm that S(IV) in the reaction solution during illumination can quantitatively convert photochemically produced NO_2 to NO_2^-, allowing the Griess spectrophotometric technique to quantify both channels of nitrate photolysis.

We can also use our Fig. 1 data to estimate the value for k_{other}, the pseudo-first-order rate constant for NO_2 loss due to other pathways, i.e., not reacting with S(IV). Combining Eqs. (5) and (6) yields

$$\phi\left(NO_2^-\right)_{(SIV)} = \phi\left(NO_2^-\right) + \phi\left(NO_2\right) \times \frac{k_{HSO_3^- + NO_2} \times \left[HSO_3^-\right] + k_{SO_3^{2-} + NO_2} \times \left[SO_3^{2-}\right]}{k_{HSO_3^- + NO_2} \times \left[HSO_3^-\right] + k_{SO_3^{2-} + NO_2} \times \left[SO_3^{2-}\right] + k_{other}}. \quad (8)$$

Fitting this equation to our data using Python (Van Rossum and Drake, 1995) yields the solid line in Fig. 1 and parameter values of $k_{other} = 700 \pm 300\ s^{-1}$, $\phi(NO_2) = (0.94 \pm 0.07)$ %, and $\phi(NO_2^-) = (1.10 \pm 0.06)$ %. We can use the value of k_{other} in Eq. (6) to calculate the percent of NO_2 that is converted to NO_2^- in solutions at a given S(IV) concentration and pH value: values are 96 %, 98 %, and 99 % at 500, 1000, and 1500 µM S(IV), respectively, at pH 8.

3.3 Addition of S(IV) after illumination

Our experiments above used S(IV) in the illumination solution to convert NO_2 to NO_2^-. While this method works, it has the disadvantage that S(IV) might interfere with other reactive species or reaction pathways during illumination. To avoid this problem, in this section we examine whether we can prevent NO_2 from escaping the sample container and convert it to nitrite by adding S(IV) to the solution after illumination.

We made several changes to the procedure in Sect. 3.2 to ensure full conversion of NO_2 to NO_2^- when adding S(IV) after illumination. We examined the effectiveness of the potential changes based on a single trial where we tested three different treatments of the samples post-illumination: (1) adding 1.5 mM S(IV) to the samples and allowing them to stir for 30 min in the dark, (2) adding 1.0 mM S(IV) and stirring for 30 min, and (3) adding 1.5 mM S(IV) and stirring for 10 min. In each case, we added the S(IV) immediately after the end of sample illumination by injecting a small volume, 25 or 38 µL, of a 33 mM sodium sulfite stock solution through the septum of the HPLC cap with a syringe and hypodermic needle. The goal with this technique is to keep the illumination container sealed so that NO_2 could not escape. Measured values of $\phi(NO_2^-)_{S(IV)}$ were (1.97 ± 0.24) %, (1.53 ± 0.19) %, and (1.60 ± 0.45) % for treatments 1, 2, and 3, respectively. The only trial that seemed to completely convert all the NO_2 to NO_2^- was the first treatment, i.e., 1.5 mM S(IV) with 30 min of stirring. As such, we used this treatment method going forward.

We also estimated the timescale of NO_2 conversion to nitrite to compare with our experimental results. Based on the volumes in the reaction vial (800 µL of solution and ~ 1.3 mL of headspace), Henry's law predicts (at 293 K) that 10 % of NO_2 should be in the aqueous phase and 90 % in the headspace. Based on the kinetic data from Clifton et al. (1988), the lifetime of total NO_2 in the vial is approximately 1 ms. This means that there should have been no difference between the results of treatments 1 and 3, which is not the case. It is unclear why there is a discrepancy between the theoretical and experimental timescales for the conversion of NO_2 to NO_2^-.

Next, we examined whether the addition of S(IV) after illumination produced results that were the same as those for experiments where S(IV) was in the solution during illumination. We performed triplicate experiments measuring the combined $NO_2 + NO_2^-$ quantum yield in pH 5 solution containing 50 µM $NaNO_3$ and 50 µM 2-propanol, as well as 1.5 mM S(IV) added to the solution after illumination. As shown in Fig. S4, the average $\pm 1\sigma$ combined quantum yield from this set of experiments is (2.10 ± 0.08) %. This is statistically no different from the result we obtained above

when S(IV) was present in the solution during illumination, $(2.00 \pm 0.14)\,\%$ ($p = 0.32$), and no different from the literature value, $(2.17 \pm 0.52)\,\%$ ($p = 0.74$; Table S1). This indicates that we can add S(IV) after the photoproduction of nitrogen dioxide has stopped and still convert all the NO_2 to NO_2^-.

3.4 Applying the S(IV) method: impact of an •OH scavenger

Our final step is to show the utility of determining both NO_2 and NO_2^- in a chemical system, by using the example of quantifying the impact of an •OH scavenger on the two channels from nitrate photolysis. Based on past work (Benedict et al., 2017; Roca et al., 2008; McFall et al., 2018), •OH can react with NO_2^- to form NO_2 in the absence of a hydroxyl radical scavenger:

$$\bullet OH + NO_2^- \rightarrow NO_2 + OH^-. \quad \text{(R4)}$$

Because of this reaction, in the absence of an •OH scavenger, the NO_2^- quantum yield should be underestimated, and the NO_2 quantum yield should be overestimated by an equal amount. In contrast, adding a scavenger suppresses the hydroxyl radical concentration and its impact on both photoproducts, giving the true quantum yield for each channel. However, we expect that the combined quantum yield, i.e., the sum of values for both channels, will be the same regardless of the presence of •OH scavengers. That is, we expect that an •OH scavenger will prevent the conversion of NO_2^- to NO_2 but will not alter the overall photochemical efficiency of nitrate photolysis. While the impact of •OH scavengers on the nitrite channel has been examined previously, we are unaware of any past attempts to measure both channels in the presence and absence of scavengers.

As shown by the blue arrow in Fig. 2, the addition of an •OH scavenger increases the NO_2^- quantum yield (by 0.14 %), as expected since it impedes the oxidation of nitrite by the hydroxyl radical (Reaction R4). Also consistent with our model above, the red arrow shows that the •OH scavenger decreases the quantum yield of the NO_2 channel (by 0.14 %), a result of the suppression of nitrite oxidation by •OH to make NO_2. The NO_2^- quantum yields without S(IV), with and without 2-propanol, are statistically different ($p = 0.04$). However, when S(IV) is added to the solution, the presence or absence of an •OH scavenger has no impact ($p = 0.95$) on the sum of the quantum yields for the two channels. This is what we expect, because the NO_2 that was formed from the reaction of •OH and NO_2^- is converted back to NO_2^- by S(IV), resulting in the same total amount of $NO_2^- + NO_2$ in the two sets of experiments. This shows that the addition of a •OH scavenger does not impact the overall efficiency of nitrate photolysis (i.e., the sum of the quantum yields of the two channels) but prevents the oxidation of NO_2^- to NO_2.

Our quantum yields in this set of experiments are in good agreement with previously determined values. As mentioned

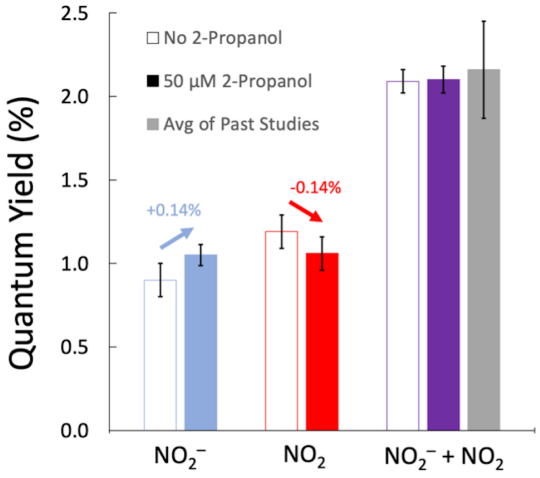

Figure 2. Measured quantum yields of nitrite (blue bars), nitrogen dioxide (red bars), and both products (purple bars) from the photolysis of 50 µM NO_3^- at 293 K and pH 5. The unfilled bars are experiments without 2-propanol (an •OH scavenger), while filled bars represent experiments with 50 µM 2-propanol. The grey bar is the sum of the average quantum yields for the two channels from past studies (Table S1). Arrows above the NO_2^- and NO_2 channels indicate the impact of the •OH scavenger. Error bars are $\pm 1\sigma$. Errors for the NO_2^- and $(NO_2^- + NO_2)$ quantum yields were calculated from replicate experiments; these errors were propagated to determine the error for the NO_2 channel result.

in Sect. 3.2, our nitrite quantum yield without S(IV) agrees with previously reported $\phi(NO_2^-)$ values. Our combined quantum yield values, $\phi(NO_2^-)_{S(IV)}$, are $(2.10 \pm 0.08)\,\%$ and $(2.09 \pm 0.16)\,\%$ with and without an •OH scavenger, respectively (Fig. 2). Our values here agree with the Table S1 average of previously determined combination of both channels, $(2.17 \pm 0.52)\,\%$ ($p > 0.70$). The NO_2 channel was calculated, using Eq. (7), as the difference in the quantum yield between experiments with S(IV) added after illumination and experiments without S(IV). In this set of experiments, our measured $\phi(NO_2)$, $(1.05 \pm 0.10)\,\%$, is similar to the average of the literature values, $(1.19 \pm 0.29)\,\%$ ($p = 0.47$), as shown in Table S1.

4 Impacts and implications

We have demonstrated that S(IV) can convert aqueous NO_2 to NO_2^-, which allows the production of both the gas- and aqueous-phase products of nitrate photolysis to be quantified in the aqueous phase in a sealed container using the same analytical method. Although nitrate photolysis is traditionally considered a minor source of NO_x, recent research has shown that the efficiency of nitrate photolysis can be enhanced by other light-absorbing compounds or its physical environment (Y. Wang et al., 2021; Mora Garcia et al., 2021; McFall et al., 2018). It is important to understand whether an apparent enhancement impacts only one channel, both chan-

nels, or is due simply to a conversion of one product to another. As many field studies have noted that the measured enhancement impacts the NO_2^- channel more than the NO_2 channel, it is likely that different chemicals impact nitrate photolysis in a variety of ways (Andersen et al., 2023; Kasibhatla et al., 2018; Ye et al., 2016). Understanding how different variables impact nitrate photolysis will allow a more comprehensive understanding of nitrogen cycling and should improve model predictions of ambient NO_x and HONO concentrations. Performing experiments with and without S(IV) for a given experimental condition will allow laboratory experiments to determine both channels of nitrate photolysis, which will reveal whether one or both channels are enhanced or if secondary chemistry is converting one product to the other.

This new S(IV) method also has applications beyond nitrate photolysis, as it can be used for any system where NO_2 needs to be quantified. This could include studies where NO_2 production occurs in the aqueous phase, such as the decomposition of metallic nitrate compounds (Gallagher et al., 1971; Yuvaraj et al., 2003) or in studies where the production of NO_2 is small enough that it cannot be quantified by commercially available analyzers.

Code and data availability. All data and code can be obtained by emailing the corresponding author at canastasio@ucdavis.edu.

Supplement. The supplement related to this article is available online at: https://doi.org/10.5194/acp-24-4411-2024-supplement.

Author contributions. AL and CA conceptualized the study, while AL, JP, and MO performed the experiments. AL performed the coding and data analysis. AL wrote the paper with input from CA.

Competing interests. The contact author has declared that none of the authors has any competing interests.

Disclaimer. Publisher's note: Copernicus Publications remains neutral with regard to jurisdictional claims made in the text, published maps, institutional affiliations, or any other geographical representation in this paper. While Copernicus Publications makes every effort to include appropriate place names, the final responsibility lies with the authors.

Acknowledgements. We appreciate the helpful comments of the anonymous reviewers.

Financial support. This research was supported by the National Science Foundation (grant no. CHE-2305164) and the California Agricultural Experiment Station (Project CA-D-LAW-6403-RR).

Review statement. This paper was edited by Sergey A. Nizkorodov and reviewed by two anonymous referees.

References

Acker, K., Möller, D., Wieprecht, W., Meixner, F. X., Bohn, B., Gilge, S., Plass-Dülmer, C., and Berresheim, H.: Strong daytime production of OH from HNO_2 at a rural mountain site, Geophys. Res. Lett., 33, L02809, https://doi.org/10.1029/2005GL024643, 2006.

Anastasio, C., Faust, B., and Allen, J.: Aqueous phase photochemical formation of hydrogen peroxide in authentic cloud waters, J. Geophys. Res.-Atmos., 99, 8231–8248, https://doi.org/10.1029/94JD00085, 1994.

Andersen, S. T., Carpenter, L. J., Reed, C., Lee, J. D., Chance, R., Sherwen, T., Vaughan, A. R., Stewart, J., Edwards, P. M., Bloss, W. J., Sommariva, R., Crilley, L. R., Nott, G. J., Neves, L., Read, K., Heard, D. E., Seakins, P. W., Whalley, L. K., Boustead, G. A., Fleming, L. T., Stone, D., and Fomba, K. W.: Extensive field evidence for the release of HONO from the photolysis of nitrate aerosols, Sci. Adv., 9, eadd6266, https://doi.org/10.1126/sciadv.add6266, 2023.

Armbruster, D. A. and Pry, T.: Limit of Blank, Limit of Detection and Limit of Quantitation, Clin. Biochem. Rev., 29, S49–S52, 2008.

Benedict, K. B., McFall, A. S., and Anastasio, C.: Quantum Yield of Nitrite from the Photolysis of Aqueous Nitrate above 300 nm, Environ. Sci. Technol., 51, 4387–4395, https://doi.org/10.1021/acs.est.6b06370, 2017.

Chu, L. and Anastasio, C.: Quantum Yields of Hydroxyl Radical and Nitrogen Dioxide from the Photolysis of Nitrate on Ice, J. Phys. Chem. A, 107, 9594–9602, https://doi.org/10.1021/jp0349132, 2003.

Clifton, C. L., Altstein, N., and Huie, R. E.: Rate constant for the reaction of nitrogen dioxide with sulfur(IV) over the pH range 5.3–13, Environ. Sci. Technol., 22, 586–589, https://doi.org/10.1021/es00170a018, 1988.

Doane, T. A. and Horwath, W. R.: Spectrophotometric Determination of Nitrate with a Single Reagent, Analyt. Lett., 36, 2713–2722, https://doi.org/10.1081/AL-120024647, 2003.

Frey, M. M., Brough, N., France, J. L., Anderson, P. S., Traulle, O., King, M. D., Jones, A. E., Wolff, E. W., and Savarino, J.: The diurnal variability of atmospheric nitrogen oxides (NO and NO_2) above the Antarctic Plateau driven by atmospheric stability and snow emissions, Atmos. Chem. Phys., 13, 3045–3062, https://doi.org/10.5194/acp-13-3045-2013, 2013.

Galbavy, E. S., Ram, K., and Anastasio, C.: 2-Nitrobenzaldehyde as a chemical actinometer for solution and ice photochemistry, J. Photochem. Photobiol. A, 209, 186–192, https://doi.org/10.1016/j.jphotochem.2009.11.013, 2010.

Gallagher, P. K., Schrey, F., and Prescott, B.: The thermal decomposition of aqueous manganese (II) nitrate solution, Thermochim.

Acta, 2, 405–412, https://doi.org/10.1016/0040-6031(71)85016-5, 1971.

Goldstein, S. and Rabani, J.: Mechanism of Nitrite Formation by Nitrate Photolysis in Aqueous Solutions: The Role of Peroxynitrite, Nitrogen Dioxide, and Hydroxyl Radical, J. Am. Chem. Soc., 129, 10597–10601, https://doi.org/10.1021/ja073609+, 2007.

Kasibhatla, P., Sherwen, T., Evans, M. J., Carpenter, L. J., Reed, C., Alexander, B., Chen, Q., Sulprizio, M. P., Lee, J. D., Read, K. A., Bloss, W., Crilley, L. R., Keene, W. C., Pszenny, A. A. P., and Hodzic, A.: Global impact of nitrate photolysis in sea-salt aerosol on NO_x, OH, and O_3 in the marine boundary layer, Atmos. Chem. Phys., 18, 11185–11203, https://doi.org/10.5194/acp-18-11185-2018, 2018.

Lee, Y. N. and Schwartz, S. E.: Kinetics of oxidation of aqueous sulfur(IV) by nitrogen dioxide, Brookhaven National Lab., Upton, NY, USA, https://wpw.bnl.gov/schwartz/wp-content/uploads/sites/11/2022/04/lee83no2sivc.pdf (last access: 12 April 2024), 1982.

Li, X., Rohrer, F., Hofzumahaus, A., Brauers, T., Häseler, R., Bohn, B., Broch, S., Fuchs, H., Gomm, S., Holland, F., Jäger, J., Kaiser, J., Keutsch, F. N., Lohse, I., Lu, K., Tillmann, R., Wegener, R., Wolfe, G. M., Mentel, T. F., Kiendler-Scharr, A., and Wahner, A.: Missing Gas-Phase Source of HONO Inferred from Zeppelin Measurements in the Troposphere, Science, 344, 292–296, https://doi.org/10.1126/science.1248999, 2014.

Lian, Z., Li, G., Zhang, S., Ma, W., and Zhong, Q.: Mechanism and Kinetic Study of Cyclodextrin Use to Facilitate NO2 Absorption in Sulfite Solutions, Environ. Sci. Technol., 56, 7696–7706, https://doi.org/10.1021/acs.est.2c00838, 2022.

Liang, Z., Zhang, R., Gen, M., Chu, Y., and Chan, C. K.: Nitrate Photolysis in Mixed Sucrose–Nitrate–Sulfate Particles at Different Relative Humidities, J. Phys. Chem. A, 125, 3739–3747, https://doi.org/10.1021/acs.jpca.1c00669, 2021.

Ma, Q., Zhong, C., Ma, J., Ye, C., Zhao, Y., Liu, Y., Zhang, P., Chen, T., Liu, C., Chu, B., and He, H.: Comprehensive Study about the Photolysis of Nitrates on Mineral Oxides, Environ. Sci. Technol., 55, 8604–8612, https://doi.org/10.1021/acs.est.1c02182, 2021.

McFall, A. S., Edwards, K. C., and Anastasio, C.: Nitrate Photochemistry at the Air–Ice Interface and in Other Ice Reservoirs, Environ. Sci. Technol., 52, 5710–5717, https://doi.org/10.1021/acs.est.8b00095, 2018.

Moorcroft, M. J., Davis, J., and Compton, R. G.: Detection and determination of nitrate and nitrite: a review, Talanta, 54, 785–803, https://doi.org/10.1016/S0039-9140(01)00323-X, 2001.

Mora Garcia, S. L., Pandit, S., Navea, J. G., and Grassian, V. H.: Nitrous Acid (HONO) Formation from the Irradiation of Aqueous Nitrate Solutions in the Presence of Marine Chromophoric Dissolved Organic Matter: Comparison to Other Organic Photosensitizers, ACS Earth Space Chem., 5, 3056–3064, https://doi.org/10.1021/acsearthspacechem.1c00292, 2021.

Pratt, P. F., Nithipatikom, K., and Campbell, W. B.: Simultaneous Determination of Nitrate and Nitrite in Biological Samples by Multichannel Flow Injection Analysis, Analyt. Biochem., 231, 383–386, https://doi.org/10.1006/abio.1995.0067, 1995.

Ridnour, L. A., Sim, J. E., Hayward, M. A., Wink, D. A., Martin, S. M., Buettner, G. R., and Spitz, D. R.: A Spectrophotometric Method for the Direct Detection and Quantitation of Nitric Oxide, Nitrite, and Nitrate in Cell Culture Media, Analyt. Biochem., 281, 223–229, https://doi.org/10.1006/abio.2000.4583, 2000.

Roca, M., Zahardis, J., Bone, J., El-Maazawi, M., and Grassian, V. H.: 310 nm Irradiation of Atmospherically Relevant Concentrated Aqueous Nitrate Solutions: Nitrite Production and Quantum Yields, J. Phys. Chem. A, 112, 13275–13281, https://doi.org/10.1021/jp809017b, 2008.

Romer, P. S., Wooldridge, P. J., Crounse, J. D., Kim, M. J., Wennberg, P. O., Dibb, J. E., Scheuer, E., Blake, D. R., Meinardi, S., Brosius, A. L., Thames, A. B., Miller, D. O., Brune, W. H., Hall, S. R., Ryerson, T. B., and Cohen, R. C.: Constraints on Aerosol Nitrate Photolysis as a Potential Source of HONO and NO_x, Environ. Sci. Technol., 52, 13738–13746, https://doi.org/10.1021/acs.est.8b03861, 2018.

Scharko, N. K., Berke, A. E., and Raff, J. D.: Release of Nitrous Acid and Nitrogen Dioxide from Nitrate Photolysis in Acidic Aqueous Solutions, Environ. Sci. Technol., 48, 11991–12001, https://doi.org/10.1021/es503088x, 2014.

Seinfeld, J. H. and Pandis, S. N.: Atmospheric Chemistry and Physics: From Air Pollution to Climate Change, 2nd Edn., John Wiley & Sons, Inc., Hoboken, NJ, 1203 pp., ISBN 13:978-0-471-72018-8, ISBN 10:0-471-72018-6, 2006.

Shen, C. H. and Rochelle, G. T.: Nitrogen Dioxide Absorption and Sulfite Oxidation in Aqueous Sulfite, Environ. Sci. Technol., 32, 1994–2003, https://doi.org/10.1021/es970466q, 1998.

Shi, Q., Tao, Y., Krechmer, J. E., Heald, C. L., Murphy, J. G., Kroll, J. H., and Ye, Q.: Laboratory Investigation of Renoxification from the Photolysis of Inorganic Particulate Nitrate, Environ. Sci. Technol., 55, 854–861, https://doi.org/10.1021/acs.est.0c06049, 2021.

Song, H., Lu, K., Ye, C., Dong, H., Li, S., Chen, S., Wu, Z., Zheng, M., Zeng, L., Hu, M., and Zhang, Y.: A comprehensive observation-based multiphase chemical model analysis of sulfur dioxide oxidations in both summer and winter, Atmos. Chem. Phys., 21, 13713–13727, https://doi.org/10.5194/acp-21-13713-2021, 2021.

Stavrakou, T., Müller, J.-F., Boersma, K. F., van der A, R. J., Kurokawa, J., Ohara, T., and Zhang, Q.: Key chemical NO_x sink uncertainties and how they influence top-down emissions of nitrogen oxides, Atmos. Chem. Phys., 13, 9057–9082, https://doi.org/10.5194/acp-13-9057-2013, 2013.

Van Rossum, G. and Drake Jr., F. L.: Python reference manual, Centrum voor Wiskunde en Informatica, Amsterdam, https://ir.cwi.nl/pub/5007/05007D.pdf (last access: 12 April 2024), 1995.

Wang, J., Li, J., Ye, J., Zhao, J., Wu, Y., Hu, J., Liu, D., Nie, D., Shen, F., Huang, X., Huang, D. D., Ji, D., Sun, X., Xu, W., Guo, J., Song, S., Qin, Y., Liu, P., Turner, J. R., Lee, H. C., Hwang, S., Liao, H., Martin, S. T., Zhang, Q., Chen, M., Sun, Y., Ge, X., and Jacob, D. J.: Fast sulfate formation from oxidation of SO_2 by NO_2 and HONO observed in Beijing haze, Nat. Commun., 11, 2844, https://doi.org/10.1038/s41467-020-16683-x, 2020.

Wang, X., Dalton, E. Z., Payne, Z. C., Perrier, S., Riva, M., Raff, J. D., and George, C.: Superoxide and Nitrous Acid Production from Nitrate Photolysis Is Enhanced by Dissolved Aliphatic Organic Matter, Environ. Sci. Technol. Lett., 8, 53–58, https://doi.org/10.1021/acs.estlett.0c00806, 2021.

Wang, Y., Huang, D. D., Huang, W., Liu, B., Chen, Q., Huang, R., Gen, M., Mabato, B. R. G., Chan, C. K., Li, X., Hao, T., Tan, Y., Hoi, K. I., Mok, K. M., and Li, Y. J.: Enhanced Nitrite

Production from the Aqueous Photolysis of Nitrate in the Presence of Vanillic Acid and Implications for the Roles of Light-Absorbing Organics, Environ. Sci. Technol., 55, 15694–15704, https://doi.org/10.1021/acs.est.1c04642, 2021.

Warneck, P. and Wurzinger, C.: Product quantum yields for the 305-nm photodecomposition of nitrate in aqueous solution, J. Phys. Chem., 92, 6278–6283, https://doi.org/10.1021/j100333a022, 1988.

Ye, C., Gao, H., Zhang, N., and Zhou, X.: Photolysis of Nitric Acid and Nitrate on Natural and Artificial Surfaces, Environ. Sci. Technol., 50, 3530–3536, https://doi.org/10.1021/acs.est.5b05032, 2016.

Ye, C., Zhang, N., Gao, H., and Zhou, X.: Photolysis of Particulate Nitrate as a Source of HONO and NO_x, Environ. Sci. Technol., 51, 6849–6856, https://doi.org/10.1021/acs.est.7b00387, 2017.

Yuvaraj, S., Fan-Yuan, L., Tsong-Huei, C., and Chuin-Tih, Y.: Thermal Decomposition of Metal Nitrates in Air and Hydrogen Environments, J. Phys. Chem. B, 107, 1044–1047, https://doi.org/10.1021/jp026961c, 2003. ’

Zellner, R., Exner, M., and Herrmann, H.: Absolute OH quantum yields in the laser photolysis of nitrate, nitrite and dissolved H_2O_2 at 308 and 351 nm in the temperature range 278–353 K, J. Atmos. Chem., 10, 411–425, https://doi.org/10.1007/BF00115783, 1990.

Zepp, R. G., Hoigné, J., and Bader, H.: Nitrate-induced photooxidation of trace organic chemicals in water, Environ. Sci. Technol., 21, 443–450, https://doi.org/10.1021/es00159a004, 1987.

Zhou, X., Civerolo, K., Dai, H., Huang, G., Schwab, J., and Demerjian, K.: Summertime nitrous acid chemistry in the atmospheric boundary layer at a rural site in New York State, J. Geophys. Res.-Atmos., 107, ACH 13-1–ACH 13-11, https://doi.org/10.1029/2001JD001539, 2002.

Zhou, X., Gao, H., He, Y., Huang, G., Bertman, S. B., Civerolo, K., and Schwab, J.: Nitric acid photolysis on surfaces in low-NO_x environments: Significant atmospheric implications, Geophys. Res. Lett., 30, 2217, https://doi.org/10.1029/2003GL018620, 2003.

Supplement of Atmos. Chem. Phys., 24, 4411–4419, 2024
https://doi.org/10.5194/acp-24-4411-2024-supplement

Atmospheric Chemistry and Physics
Open Access
EGU

Supplement of

Technical Note: A technique to convert NO_2 to NO_2^- with S(IV) and its application to measuring nitrate photolysis

Aaron Lieberman et al.

Correspondence to: Cort Anastasio (canastasio@ucdavis.edu)

Table of Contents

Section S1. Materials and Solution Preparation

Sodium nitrate (ACS grade), sodium sulfite (ACS grade), 2-propanol (ACS plus grade), potassium phosphate monobasic (ACS grade), sodium hydroxide (ACS grade), and hydrochloric acid (trace metal grade) were purchased from Fisher Scientific. Sodium nitrite (99.9995%) was purchased from Thermos Scientific. Sulfanilamide (99%), N-(1-napthyl)ethylenediamine dihydrochloride (NED) (reagent grade), and hydrogen peroxide (H_2O_2) (30% solution) were purchased from Sigma Aldrich.

All solutions were prepared with water from a Milli-Q (MQ) Advantage A10 system (18.2 MΩ cm) with an upstream carbon cartridge (Barnstead) that kept TOC < 5 ppb. Illumination solutions were prepared with 50 µM sodium nitrate, 50 µM 2-propanol (as an $^{\bullet}OH$ scavenger) and varying concentrations of sodium sulfite. The illumination solutions were either prepared in MQ water or in a pH 8 phosphate buffer (0.010 M potassium phosphate monobasic in MQ water) where the pH was adjusted with sodium hydroxide or hydrochloric acid. Standards were prepared with sodium nitrite and contained the same concentration of S(IV) as the illumination solution. The Griess color development method was performed with either: (1) 25 µL of 1% (w/v) sulfanilamide in 10% (v/v) HCl/MQ solution and 25 µL of 0.1% (w/v) NED solution or (2) 50 µL of 1% (w/v) sulfanilamide in 30% (v/v) HCl/MQ and 50 µL of 0.1% (w/v) NED solution if the solution contained sulfite. Hydrogen peroxide was added to convert S(IV) to S(VI) in the reaction solutions and nitrite standards. Since H_2O_2 in the stock solution slowly decays, we monitored the concentration daily with a Shimadzu UV-2501PC spectrophotometer by monitoring the absorbance at 240 nm and using the base-10 molar absorption coefficient of 38.1 M^{-1} cm^{-1} (Miller and Kester, 1988). The Dionex check standard was made from the Dionex Combined Seven Anion Standard II diluted to 100-130 nM NO_2^-.

Illumination solutions were prepared from stock solutions of 0.10 M sodium nitrate, 0.10 M 2-propanol and 0.033 M sodium sulfite. The stock solutions of sodium nitrate and 2-propanol were prepared biannually and stored in amber bottles in a refrigerator. Both the sodium sulfite solutions and sodium nitrite standard curve standards were made fresh daily from their respective salt. The sulfanilamide and NED solutions were prepared monthly.

Section S2. Adapting the Griess Method for the Presence of Sulfite

A major problem with using S(IV) to convert NO_2 to NO_2^- is that S(IV) not only reacts with NO_2, but also other chemicals in solution. As shown in Figure S1, the addition of S(IV) to nitrite standards inhibits the Griess method of analysis by preventing the formation of the azo-dye, rendering spectroscopic analysis impossible. In contrast, sulfate, i.e., S(VI), does not interfere with the analysis of nitrite (Fig. S1). Therefore, oxidizing S(IV) to S(VI) after the conversion of NO_2 to NO_2^- but prior to the addition of the sulfanilamide reagent should allow us to accurately measure both nitrite and nitrogen dioxide production. We tried two different methods of oxidation: bubbling air into the solution and adding H_2O_2. Although bubbling air reduces the interference of S(IV) on nitrite determination, the relative standard error across replicate 100 nM NO_2^- standards is large (34%), and therefore this is not an appropriate method. In contrast, adding H_2O_2 to standard curve solutions containing S(IV) prior to the start of the Griess analysis effectively reduces the interference of S(IV) on nitrite measurements. The nitrite calibration

curve regression line is linear and the 100 nM NO_2^- replicates are within 3% of each other. Therefore, we are able to measure nitrite in the presence of S(IV) by oxidizing the S(IV) to S(VI) with H_2O_2.

We then tested how the molar ratio of H_2O_2:S(IV) impacts both the linearity of the standard curve and the relative error among replicate standards. We tested molar ratios of 0.5:1, 1:1, 2:1, and 3:1 H_2O_2:S(IV). Both the 1:1 and 2:1 ratio standard curves have an R^2 greater than 0.99 while the corresponding values for the 0.5:1 and 3:1 ratio standard curves were less than 0.98. The 2:1 ratio provided triplicate 100 nM standard measurements that are within 5% of the true value and each other, while the 1:1: ratio 100 nM standard triplicates are within 15% of each other and the true value. Based on the excellent calibration curve linearity and replicate reproducibility, we use a 2:1 molar ratio of H_2O_2:S(IV).

We find that the nitrite signal in the presence of S(IV) and H_2O_2 is time sensitive, decaying by approximately 15% over the course of ~40 minutes after the addition of the NED solution. After this time, the error in the replicate standard and check standard are both greater than 10%, while after 4 hours there is no nitrite signal. We resolved this problem by immediately starting the UV-VIS analysis after waiting the necessary 10 minutes post NED addition, and by collecting all the UV-VIS spectra for a given set of samples within 20 minutes of recording the first sample spectrum. We also test both a 100 nM NO_2^- replicate standard and the Dionex check at the start and end of each batch of 8-10 samples to ensure that the signal does not change more than 10% throughout the analysis.

As shown in Figure S2, as the S(IV) concentration increases, the slope of the nitrite calibration curve regression line decreases. This could either be because of higher H_2O_2 (since we maintained a H_2O_2:S(IV) ratio of 2:1) or because of higher residual S(IV) after H_2O_2 addition. Although we are unsure whether S(IV), H_2O_2, or both are reacting with the sulfanilamide and/or NED reagents, we found that doubling the volume of the sulfanilamide and NED added to the samples produces a more linear calibration curve.

Another concern was that H_2O_2 could react with either nitrite, to form peroxynitrite, or the azo-dye, artificially decreasing the measured concentration of nitrite. However, we do not believe this is occurring under our conditions for the following reasons. In a pH 5 solution with 100 nM NO_2^- and 3 mM H_2O_2, the lifetime of NO_2^- is ~8.5 hours (~6 hour half-life) and the peroxynitrite formation rate would be 3.3 pM s^{-1} (Lukes et al., 2014). Since the azo-dye is formed from the Griess analysis within 20 minutes of the addition of H_2O_2, less than 5% of the nitrite would react with H_2O_2 during this time period. As discussed in section S3, we found the stability of the azo-dye to be 5 hours in the presence of H_2O_2. As long as the samples are analyzed within this 5-hour window, there should be no measurable destruction of the azo-dye by H_2O_2.

Because of the impact of S(IV) on the nitrite response, the calibration curve on a given day needs to contain the same S(IV) and H_2O_2 concentrations as the experimental solutions. With this procedure, the Dionex check standard and standard replicate give nitrite concentrations within 15% of their actual values, indicating that we can correct for the impacts of S(IV) and H_2O_2 on the nitrite response. However, the interference from S(IV) could be a problem at higher concentrations if the nitrite calibration curve becomes so flat that the regression line loses the required resolution for nitrite analysis.

Our final adaptation to the standard Griess method of analysis is in response to the effect of S(IV) on pH. The reaction of nitrite with Griess reagents to form the light-absorbing azo dye requires a pH below 2. Since the addition of 1.5 mM of Na_2SO_3 prevented the solution from becoming that acidic, we increased the acidity of the sulfanilamide solution from 10% to 30% hydrochloric acid, as recommend by Doane and Horwath (2003).

Section S3. Stability of Adapted Griess Reagent Samples

Here we consider the stability of the samples from sample treatments 1-3, which are described in Section 2.3 of the main text. The stability for sample treatment 1, i.e,. no S(IV) in solution, is known and the following considerations must be made. Once the nitrite has been generated in solution, the sample is stable for up to 28 days if kept refrigerated at 4 ˚C, otherwise it must be analyzed within 48 hours (Roman et al., 1991). Once the sulfanilamide has been added, the diazonium ion decays by ~2-3% per hour, therefore it is recommended to add the NED solution within 15 minutes of adding the sulfanilamide (Fox, 1979). There is no mention in the literature of the stability of the azo-dye once it has been formed, but based on our experiments it is stable for at least 4 hours on benchtop but is likely stable for longer.

Sample treatment 2, where S(IV) was present in solution during the illumination, is less stable than sample treatment 1. We found that after the nitrite was produced, the samples were stable for up to one week if kept refrigerated and covered at 4 ˚C. After the addition of H_2O_2, the samples were unstable after 5 minutes, so the sulfanilamide reagent needed to be added within this time for results to be precise and accurate. We did not test the stability of the diazonium ion formed after adding the sulfanilamide reagent, but after addition of the NED reagent, the samples were stable for up to 5 hours when left on the benchtop in the dark, and were found to degrade after 6 hours.

Sample treatment 3, where S(IV) was added to solution after illumination, had the same stability as sample treatment 2, except for one key difference, the addition of S(IV). Since this sample treatment adds S(IV) after illumination, the S(IV) must be added before the NO_2 decays or escapes from the illumination container. We found that we had to immediately inject the S(IV) into solution after stopping illumination. Waiting more than five minutes to add the S(IV) significantly decreased the NO_2 recovery.

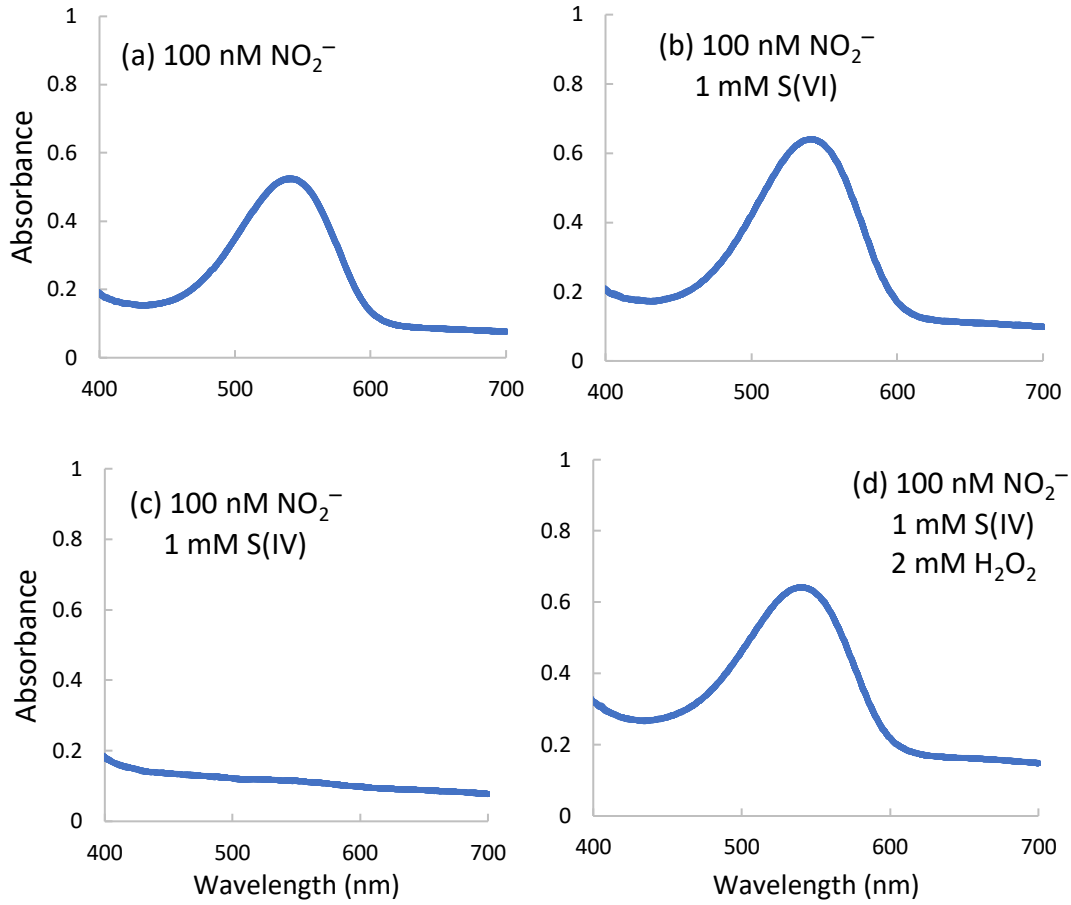

Figure S1. UV-VIS spectra for (a) 100 nM NO_2^-, (b) 100 nM NO_2^- and 1.0 mM sulfate (S(VI)), (c) 100 nM NO_2^- and 1.0 mM sulfite (S(IV)) and (d) 100 nM NO_2^-, 1.0 mM S(IV), and 2.0 mM H_2O_2. For panels (b) and (c), the sulfanilamide solution was added to start the Griess method of analysis within 5 and 10 minutes, respectively, after the preparation of the NO_2^- and S(VI) solution. For panel (d), the H_2O_2 was added within 3 min after the NO_2^- and sulfite solution was prepared, and the sulfanilamide reagent was added within 3 minutes after that.

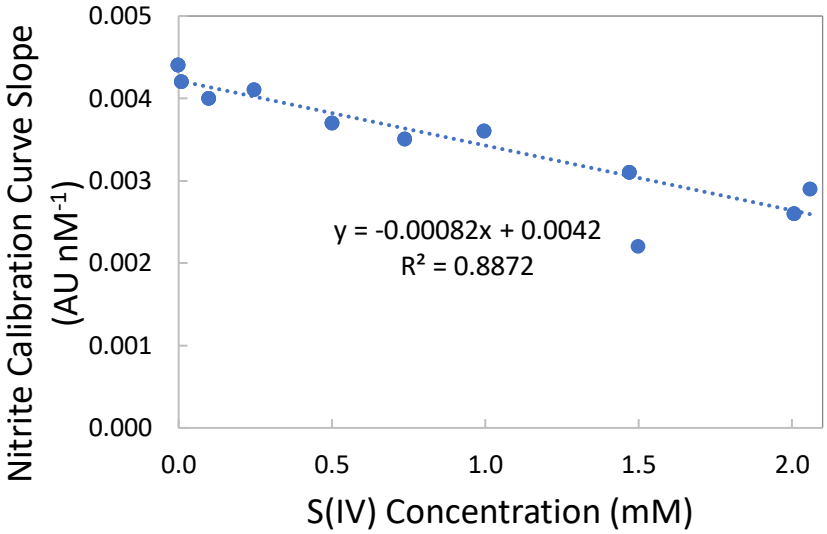

Figure S2. Impact of S(IV) concentration on the slope of the nitrite calibration curve. Each standard contained nitrite, the stated concentration of S(IV), and H_2O_2 at twice the S(IV) concentration.

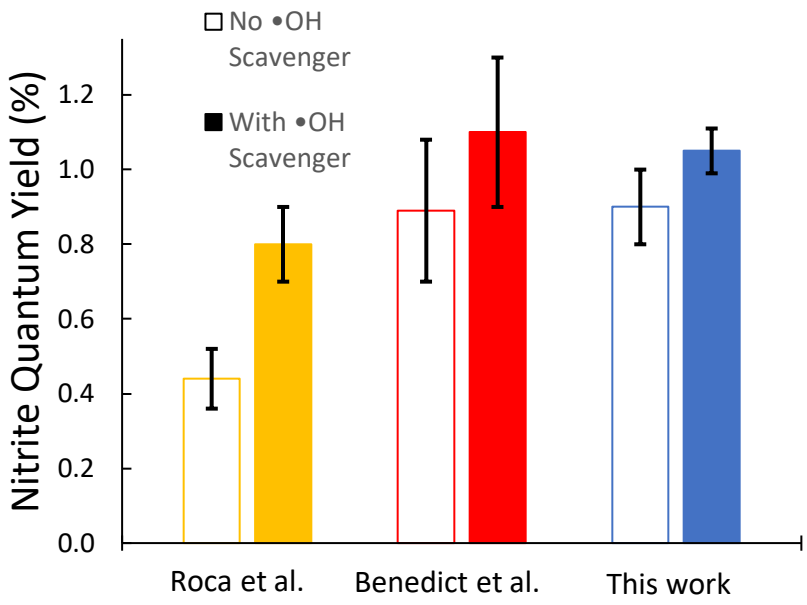

Figure S3. Influence of •OH scavenger on the nitrite quantum yield. Data are from: Roca et al. (2008) (yellow bars: 310 nm, 298 K, pH 4, 10 mM NO_3^-; no formate (hollow bar) or 10 mM formate (solid bar)); Benedict et al. (2017b) (red bars: 313 nm, 298 K, pH < 5, 50 µM NO_3^-; no formate or cysteine (hollow bar) and with 50 µM formate or cysteine (solid bar)); and this work (blue bars: 313 nm, 293 K, pH 5, 50 µM NO_3^-; no 2-propanol (hollow) or 50 µM 2-propanol (solid)). Error bars are ±1 σ for this work and Benedict et al., while the error bar for Roca et al. is their unspecified reported error.

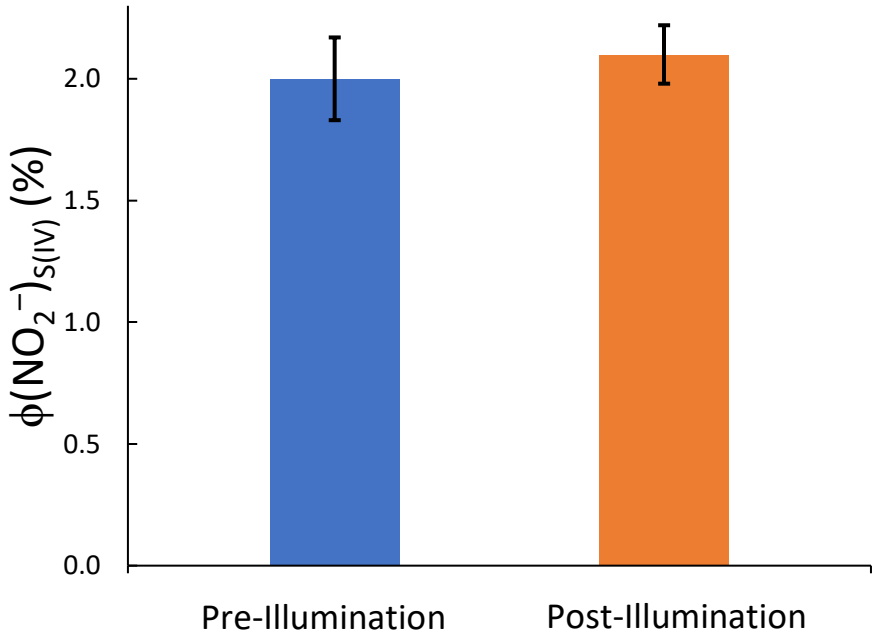

Figure S4. Comparison of the quantum yield for nitrite in the presence of S(IV) under two experimental conditions: (1) "Pre-Illumination", where 1.5 mM S(IV) was added to the solution prior to illumination or (2) "Post-Illumination", where 1.5 mM S(IV) was added after illumination. The quantum yields for the two conditions, (2.00 ± 0.14)% and (2.10 ± 0.08)%, respectively, are not statistically different (p = 0.16).

Table S1. Summary of literature values of $\Phi(NO_2)$ and $\Phi(NO_2^-)$ from aqueous nitrate photolysis

Study	Wavelength (nm)	Experiment Temp. (K)	Nitrate Concentration (μM)	Measured Quantum Yield	Quantum Yield at 293 K[a]
Determinations of hydroxyl radical quantum yields (channel 1)					
Zepp et al. (1987)	313	293	200-4000	1.30%	1.30%
Warneck & Wurzinger (1988)	305	295	10,000	0.92%	0.80%
Zellner et al. (1990)	308	298	3000	1.70%	1.50%
Chu and Anastasio (2003)	313	298	200	1.33%	1.20%
				Average (± 1 σ) $\phi(^{\bullet}OH)$ = 1.19 ± 0.29%	
Determinations of nitrite quantum yields from studies that used $^{\bullet}OH$ scavengers (channel 2)					
Warneck & Wurzinger (1988)	305	295	10,000	1.04%	1.01%
Goldstein & Rabani (2007)	300	297	20,000-100,000	0.94%	0.88%
Roca et al. (2008)	310	298	10,000	0.80%	0.74%
Benedict et al. (2017a)	313	293	50	1.14%	1.14%
Benedict et al. (2017b)	313	298	50	1.10%	1.02%
McFall et al. (2018)	313	298	50	0.93%	0.86%
				Average (± 1 σ) $\phi(NO_2^-)$ = 0.98 ± 0.11%	
				Average (± 1 σ) ($\phi(NO_2^-) + \phi(^{\bullet}OH)$) = 2.17 ± 0.52%	

[a] Quantum yields not measured at 293 K were adjusted to this temperature with the Arrhenius equation using the activation energies from Chu et al. (2003), 20 kJ/mol, and Benedict et al. (2017b), 11 kJ/mol, for $\phi(^{\bullet}OH)$ and $\phi(NO_2^-)$, respectively.

Table S2. Conditions and $\phi(NO_2^-)_{S(IV)}$ measurements for experiments in Figures 1 and 2. All illuminations were performed with 50 μM $NaNO_3$, 313 nm illumination, and a temperature of 293 K.

Expt #	2-Propanol Concentration (μM)	S(IV) Concentration (μM)	Pre- or Post-Illumination S(IV) Addition	pH	j_{2NB} (s^{-1})	$\phi(NO_2^-)$ or $\phi(NO_2^-)_{S(IV)}$ (%)
1	0	0	N/A	4.9	0.0448	1.05
2	0	0	N/A	4.9	0.0448	0.94
3	0	0	N/A	4.9	0.0448	0.92
4	0	0	N/A	4.8	0.0469	0.79
5	0	0	N/A	4.8	0.0469	0.82
6	50	0	N/A	5.0	0.0485	1.13
7	50	0	N/A	4.9	0.0489	1.04
8	50	0	N/A	4.9	0.0489	1.07
9	50	0	N/A	4.9	0.0489	0.96
10	50	10	Pre	7.0	0.0415	1.21
11	50	10	Pre	7.0	0.0415	1.49
12	50	10	Pre	7.0	0.0415	1.38
13	50	100	Pre	7.8	0.0414	1.87
14	50	100	Pre	7.8	0.0414	1.53
15	50	100	Pre	7.8	0.0414	1.84
16	50	250	Pre	8.2	0.0423	1.87
17	50	250	Pre	8.2	0.0423	1.55
18	50	500	Pre	8.3	0.0403	2.08
19	50	500	Pre	8.3	0.0403	1.79
20	50	500	Pre	8.3	0.0403	2.00
21	50	750	Pre	8.3	0.0215	2.03
22	50	750	Pre	8.3	0.0215	1.93
23	50	750	Pre	8.3	0.0215	2.30
24	50	1000	Pre	8.2	0.0427	1.90

25	50	1000	Pre	8.2	0.0427	2.00
26	50	1000	Pre	8.2	0.0427	2.00
27	50	1500	Pre	8.6	0.0471	2.10
28	50	1500	Pre	8.6	0.0471	2.07
29	50	1500	Pre	8.6	0.0471	2.11
30	50	1500	Pre	8.6	0.0471	1.81
31	50	2000	Pre	8.6	0.0403	2.00
32	50	2000	Pre	8.6	0.0403	2.02
33	50	2000	Pre	8.6	0.0403	2.06
34	50	1500	Post	5.1	0.0489	2.09
35	50	1500	Post	5.1	0.0371	2.18
36	50	1500	Post	5.0	0.0494	2.03
36	0	1500	Post	5.1	0.0425	2.23
37	0	1500	Post	5.1	0.0399	2.13
38	0	1500	Post	5.0	0.0457	1.92

References

Benedict, K. B. and Anastasio, C.: Quantum Yields of Nitrite (NO_2^-) from the Photolysis of Nitrate (NO_3^-) in Ice at 313 nm, J. Phys. Chem. A, 121, 8474–8483, https://doi.org/10.1021/acs.jpca.7b08839, 2017.

Benedict, K. B., McFall, A. S., and Anastasio, C.: Quantum Yield of Nitrite from the Photolysis of Aqueous Nitrate above 300 nm, Environ. Sci. Technol., 51, 4387–4395, https://doi.org/10.1021/acs.est.6b06370, 2017.

Chu, L. and Anastasio, C.: Quantum Yields of Hydroxyl Radical and Nitrogen Dioxide from the Photolysis of Nitrate on Ice, J. Phys. Chem. A, 107, 9594–9602, https://doi.org/10.1021/jp0349132, 2003.

Doane, T. A. and Horwath, W. R.: Spectrophotometric Determination of Nitrate with a Single Reagent, Analytical Letters, 36, 2713–2722, https://doi.org/10.1081/AL-120024647, 2003.

Fox, J. B.: Kinetics and mechanisms of the Griess reaction, Anal. Chem., 51, 1493–1502, https://doi.org/10.1021/ac50045a032, 1979.

Goldstein, S. and Rabani, J.: Mechanism of Nitrite Formation by Nitrate Photolysis in Aqueous Solutions: The Role of Peroxynitrite, Nitrogen Dioxide, and Hydroxyl Radical, J. Am. Chem. Soc., 129, 10597–10601, https://doi.org/10.1021/ja073609+, 2007.

Lukes, P., Dolezalova, E., Sisrova, I., and Clupek, M.: Aqueous-phase chemistry and bactericidal effects from an air discharge plasma in contact with water: evidence for the formation of peroxynitrite through a pseudo-second-order post-discharge reaction of H_2O_2 and HNO_2, Plasma Sources Sci. Technol., 23, 015019, https://doi.org/10.1088/0963-0252/23/1/015019, 2014.

McFall, A. S., Edwards, K. C., and Anastasio, C.: Nitrate Photochemistry at the Air–Ice Interface and in Other Ice Reservoirs, Environ. Sci. Technol., 52, 5710–5717, https://doi.org/10.1021/acs.est.8b00095, 2018.

Miller, W. L. and Kester, D. R.: Hydrogen peroxide measurement in seawater by (p-hydroxyphenyl)acetic acid dimerization, Anal. Chem., 60, 2711–2715, https://doi.org/10.1021/ac00175a014, 1988.

Roca, M., Zahardis, J., Bone, J., El-Maazawi, M., and Grassian, V. H.: 310 nm Irradiation of Atmospherically Relevant Concentrated Aqueous Nitrate Solutions: Nitrite Production and Quantum Yields, J. Phys. Chem. A, 112, 13275–13281, https://doi.org/10.1021/jp809017b, 2008.

Roman, M., Dovi, R., Yoder, R., Dias, F., and Warden, B.: Determination by ion chromatography and spectrophotometry of the effects of preservation on nitrite and nitrate, Journal of Chromatography A, 546, 341–346, https://doi.org/10.1016/S0021-9673(01)93032-8, 1991.

Warneck, P. and Wurzinger, C.: Product quantum yields for the 305-nm photodecomposition of nitrate in aqueous solution, J. Phys. Chem., 92, 6278–6283, https://doi.org/10.1021/j100333a022, 1988.

Zellner, R., Exner, M., and Herrmann, H.: Absolute OH quantum yields in the laser photolysis of nitrate, nitrite and dissolved H_2O_2 at 308 and 351 nm in the temperature range 278–353 K, J Atmos Chem, 10, 411–425, https://doi.org/10.1007/BF00115783, 1990.

Zepp, R. G., Hoigné, J., and Bader, H.: Nitrate-induced photooxidation of trace organic chemicals in water, Environ. Sci. Technol., 21, 443–450, https://doi.org/10.1021/es00159a004, 1987.